Design and performance of 10-Gb/s L-band REAM-SOA for OLT Transmitter in next generation access networks

Dong-Hun Lee,* Jong Sool Jeong, Ki-Soo Kim, Hyun-Soo Kim, Dong Churl Kim, Mi-Ran Park, Yong-Tak Han, Oh Kee Kwon, and O-Kyun Kwon

Photonic/Wireless Convergence Components Department, ETRI, 161 Gajeong-dong, Yuseong, Daejeon 305-700, South Korea
**dhlee@etri.re.kr*

Abstract: We present a 10-Gb/s L-band reflective electro-absorption modulator integrated with a semiconductor optical amplifier (REAM-SOA) having improved transmission performance at very low input power of seed light. To decrease the input power of seed light, the absorption characteristics of the REAM are adjusted to reduce the amplified spontaneous emission light returned into the SOA, suppressing the gain saturation effect of the SOA. At a considerably low input power of −16 dBm, the REAM-SOA exhibits a low transmission penalty of about 1.2 dB after 50-km SMF transmission. Over a wide input power range from −16 dBm to 5 dBm, a penalty of less than 1.6 dB is achieved at 50-km transmission.

OCIS codes: (250.5300) Photonic integrated circuits; (060.4510) Optical communications.

References and links

1. FSAN next generation PON task group, *http://www.fsan.org/task-groups/ngpon/*
2. Y. Luo, X. Zhou, F. Effenberger, X. Yan, G. Peng, Y. Qian, and Y. Ma, "Time- and Wavelength-Division Multiplexed Passive Optical Network (TWDM-PON) for Next-Generation PON Stage 2 (NG-PON2)," J. Lightwave Technol. **31**(4), 587–593 (2013).
3. D. Smith, I. Lealman, X. Chen, D. Moodie, P. Cannard, J. Dosanjh, L. Rivers, C. Ford, R. Cronin, T. Kerr, L. Johnston, R. Waller, R. Firth, A. Borghesani, R. Wyatt, and A. Poustie, "Colourless 10Gb/s reflective SOA-EAM with low polarization sensitivity for long-reach DWDM-PON networks," in *European Conference and Exhibition on Optical Communication (ECOC)*, (2009), Paper 8.6.3.
4. N. Dupuis, J. Decobert, C. Jany, F. Alexandre, A. Garreau, N. Lagay, F. Martin, D. Carpentier, J. Landreau, and C. Kazmierski, "10-Gb/s AlGaInAs colorless remote amplified modulator by selective area growth for wavelength agnostic networks," IEEE Photon. Technol. Lett. **20**(21), 1808–1810 (2008).
5. H.-S. Kim, D. C. Kim, K.-S. Kim, B.-S. Choi, and O.-K. Kwon, "10.7 Gb/s reflective electroabsorption modulator monolithically integrated with semiconductor optical amplifier for colorless WDM-PON," Opt. Express **18**(22), 23324–23330 (2010).
6. D. C. Kim, H.-S. Kim, K. S. Kim, B.-S. Choi, J.-S. Jeong, and O.-K. Kwon, "10 Gbps SOA-REAM using monolithic integration of planar buried-heterostructure SOA with deep-ridge waveguide EA Modulator for colourless optical source in WDM-PON," in European Conference and Exhibition on Optical Communication (ECOC), (2011), Paper Tu.5.LeSaleve.5.
7. K. Ławniczuk, O. Patard, R. Guillamet, N. Chimot, A. Garreau, C. Kazmierski, G. Aubin, and K. Merghem, "40-Gb/s Colorless Reflective Amplified Modulator," IEEE Photon. Technol. Lett. **25**(4), 341–343 (2013).
8. J. S. Jeong, H.-S. Kim, B.-S. Choi, D. C. Kim, K.-S. Kim, M. R. Park, and O.-K. Kwon, "Mitigation of Rayleigh crosstalk using noise suppression technique in 10-Gb/s REAM-SOA," Opt. Express **20**(24), 26373–26378 (2012).
9. N. Cheng, J. Gao, C. Xu, B. Gao, X. Wu, D. Liu, L. Wang, X. Zhou, H. Lin, and F. Effenberger, "World's first demonstration of pluggable optical transceiver modules for flexible TWDM PONs" in Proc. ECOC 2013, paper PD.4.F.4.
10. C. P. Lai, R. Vaernewyck, A. Naughton, J. Bauwelinck, X. Yin, X.Z. Qiu, G. Maxwell, D. W. Smith, A. Borghesani, R. Cronin, K. Grobe, N. Parsons, E. Kehayas, P. D. Townsend, "Multi-Channel 11.3-Gb/s Integrated Reflective Transmitter for WDM-PON", ECOC (2013), paper Tu.1.B.2.
11. A. Borghesani, "Reflective based active semiconductor components for next generation optical access networks," European Conference on Optical Communication (ECOC), (Torino, 2010), Paper Mo.1.B.1.

#226514 - $15.00 USD Received 7 Nov 2014; revised 15 Jan 2015; accepted 22 Jan 2015; published 28 Jan 2015

12. A. Naughton, C. Antony, P. Ossieur, S. Porto, G. Talli, and P. D. Townsend, "Optimisation of SOA-REAMs for Hybrid DWDM-TDMA PON Applications," Opt. Express **19**(26), B722–B727 (2011).
13. M. Itoh, Y. Shibata, T. Kakitsuka, Y. Kadota, and Y. Tohmori, "Polarization-insensitive SOA with a strained bulk active layer for network device application," IEEE Photon. Technol. Lett. **14**(6), 765–767 (2002).
14. R. Weinmann, D. Baums, U. Cebulla, H. Haisch, D. Kaiser, E. Kuhn, E. Lach, K. Satzke, J. Weber, P. Wiedemann, and E. Zielinski, "Polarization-independent and ultra-high bandwidth electroabsorption modulator in multiquantum-well deep-ridge waveguide technology," IEEE Photon. Technol. Lett. **8**(7), 891–893 (1996).
15. T. Watanabe, N. Sakaida, H. Yasaka, F. Kano, and M. Koga, "Transmission Performance of Chirp-Controlled Signal by Using Semiconductor Optical Amplifier," J. Lightwave Technol. **18**(8), 1069–1077 (2000).
16. H. N. Tan, M. Matsuura, and N. Kishi, "Enhancement of input power dynamic range for multiwavelength amplification and optical signal processing in a semiconductor optical amplifier using holding beam effect," J. Lightwave Technol. **28**(17), 2593–2602 (2010).
17. Q. T. Nguyen, L. Bramerie, P. Besnard, A. Shen, A. Garreau, C. Kazmierski, G. H. Duan, and J. C. Simon, "24 channels colorless WDM-PON with L-band 10Gb/s downstream and C-band 2.5Gb/s upstream using multiple-wavelength seeding sources based on mode-locked lasers," in *Conference on Optical Fiber Communications,* Technical Digest (CD) (Optical Society of America, 2010), paper OThG6.

1. Introduction

As the bandwidth demand continuously increases for high-quality broadband services such as IPTV/OTT, high-definition multimedia, and advanced convergence applications, new access network technologies are developed to provide the large transmission capacity. Time and wavelength division multiplexed passive optical network (TWDM-PON) and point-to-point wavelength multiplexed passive optical network (WDM-PON) technologies approved as the standard of the next generation passive optical network stage2 (NG-PON2) under Recommendation G.989.1 have been recognized as the most promising solutions to address the bandwidth demand of 10-Gb/s-per-subscriber for next-generation access networks [1, 2]. Recently, the reflective electro-absorption modulator integrated with a semiconductor optical amplifier (REAM-SOA) for 10-Gb/s operation or higher has drawn intensive attention as an attractive solution to realize both high bandwidth and wavelength agnostics [3–7]. Practically, the REAM-SOA can resolve many issues arising from the use of the tunable laser diode (TLD) and the electro-absorption modulated laser (EML), which require wavelength allocation and alignment as well as a complicated monitoring system. Therefore, many investigations for the REAM-SOA have been carried out for the development of the upstream transmitter even if it can suffer from Rayleigh back-scattering noise [8]. On the other hand, the use of the REAM-SOA for the downstream transmitter, exploited at the optical line terminal (OLT) of the central office, can significantly reduce system complexity and burden due to the intrinsic support of the wavelength agnostics, which eliminates the need for complicated equipment and procedures to monitor and align the operation wavelength to be required in the tunable transmitter using the TLD or the fixed-wavelength transmitter using the EML [9]. In addition, both EML and TLD require the elaborate and expensive fabrication process such as E-beam lithography as well as the internal wavelength stabilizer or the external wavelength alignment equipment in order to overcome the long-term wavelength-drift problem. Additionally, the REAM-SOA is considered as a key enabler for the integrated reflective multi-channel transmitter, which is capable of delivering reduction of size, energy, and cost at the OLT [10]. As the external seed-light source for the reflective-type transmitter can accommodate multiple OLTs, the reduction of the incident power into the transmitter can considerable increase the number of shared OLTs, which leads to the decrease of the system cost [11]. As illustrated in Fig. 1, the shared OLTs can be also applied to the TWDM-PON system consisted of the reflective-type transmitters and the 4-wavelength CW seed light.

In this paper, we report the development of the L-band REAM-SOA for the 10-Gb/s OLT transmitter that was designed and fabricated to achieve improved transmission performance at low input power of seed light. It is realized by adjusting the absorption characteristic of the REAM in order to reduce the amplified spontaneous emission (ASE) light returned into the SOA, which leads to the suppression of the gain saturation effect in the SOA. This approach results in a low power penalty during back-to-back operation as well as a negligible transmission penalty at 25-km distance when the optical input power is greatly reduced. For 50-km long-reach transmission, a low transmission penalty is exhibited over a wide input

#226514 - $15.00 USD Received 7 Nov 2014; revised 15 Jan 2015; accepted 22 Jan 2015; published 28 Jan 2015

power range. It is also found that the transmission distance is extended up to 75 km with error-free performance when the input power is properly controlled.

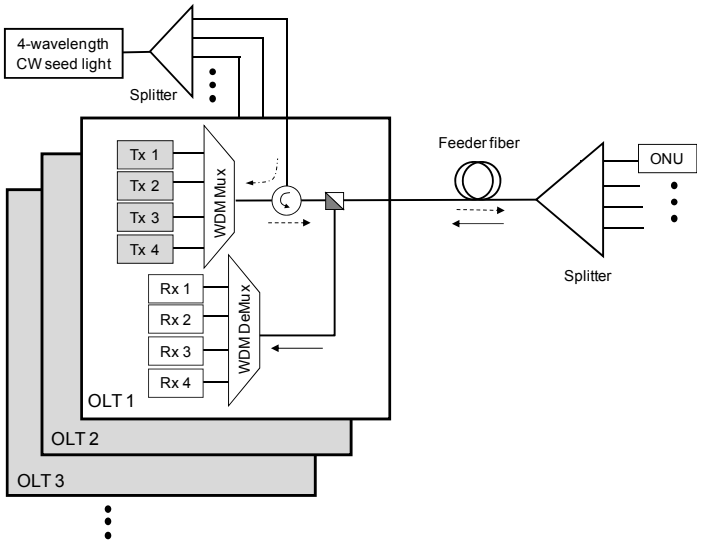

Fig. 1. TWDM-PON system diagram using the reflective-type transmitters.

2. Design and fabrication

Figure 2 shows the operation scheme and a photograph of the REAM-SOA chip. As shown in Fig. 2(a), the SOA is operated by DC for signal amplification and the REAM is modulated by RF voltage for the generation of a high-speed signal. As depicted in the schematic view of Fig. 2(a), CW seed light is injected into the device and pre-amplified by the SOA, and then modulated and reflected by the REAM. The reflected modulation signal is re-amplified by the SOA and emitted out at the front facet. In addition, the CW ASE light generated from the SOA is propagated into both directions of the SOA waveguide. Here, the ASE light toward the front facet is directly emitted out through the front facet, but the ASE light toward the rear facet is amplified and emitted out after modulation and reflection by the REAM. Thus, three different output lights of the CW ASE light, the modulated ASE light, and the modulated optical signal are emitted out through the front facet of the REAM-SOA. Here, the modulated ASE light and the modulated optical signal could give rise to carrier-density modulation by the gain saturation effect of the SOA. In particular, when the optical power of the modulated ASE light is so high that the gain saturation occurs, the signal distortions and the degradation of transmission performance can be taken place even though the power of CW seed light is sufficiently low. Naughton et al. reported the influences of the modulated ASE power reflected from the REAM by controlling the external optical attenuator between the SOA and the REAM [12]. It was found that the eye pattern distortions were more clearly observed even at very low input power when the ASE light returned into the SOA is increased by decreasing the attenuation between the SOA and the REAM. Therefore, to overcome the performance degradation of the optical signal when the optical input power is low, it is necessary to decrease the modulated ASE light returned into the SOA by exploiting a suitable REAM length and a proper wavelength deviation between the ASE center of the SOA and the absorption peak of the EAM. Figure 2(b) shows the photograph of the REAM-SOA based on an evanescent coupled double-core structure for a spot-size converter (SSC) [6]. All epitaxial layers of the REAM-SOA are grown on an n-type InP substrate by metal organic chemical vapor deposition (MOCVD). The monolithically integrated REAM-SOA was fabricated by using a two-step butt-joint regrowth technique with low loss and residual reflections. The REAM-SOA structure consists of a 600-μm-long planar buried heterostructure (PBH) SOA

#226514 - $15.00 USD Received 7 Nov 2014; revised 15 Jan 2015; accepted 22 Jan 2015; published 28 Jan 2015

with a width of 1.0 μm, a 100-μm-long high-mesa EAM waveguide with a width of 2.0 μm, and a 550-μm-long SSC. In order to obtain a low polarization dependence gain, the SOA core is fabricated by a tensile strained bulk InGaAsP layer [13]. The EAM active layer consists of nine tensile strained InGaAsP wells and ten lattice-matched InGaAsP barriers, which can decrease bias voltage and polarization dependence [14]. And the EAM mesa waveguide achieves the planarization with a 3-μm-thick benzocyclobutene (BCB) layer and the measured total capacitance of the EAM section is less than 0.2 pF. The front facet of the REAM-SOA is anti-reflection (AR) coated for ensuring low reflectivity of about 10^{-5} and the rear facet is high reflection (HR) coated for high reflectivity of about 90%. The ASE center wavelength of the SOA is positioned around 1520 nm and the absorption peak wavelength of the EAM is located around 1540 nm. The wavelength deviation between the SOA ASE center and the EAM absorption peak can increase the absorption of the ASE light emitted from the SOA as well as preserve the gain characteristics at the L-band region of the REAM-SOA.

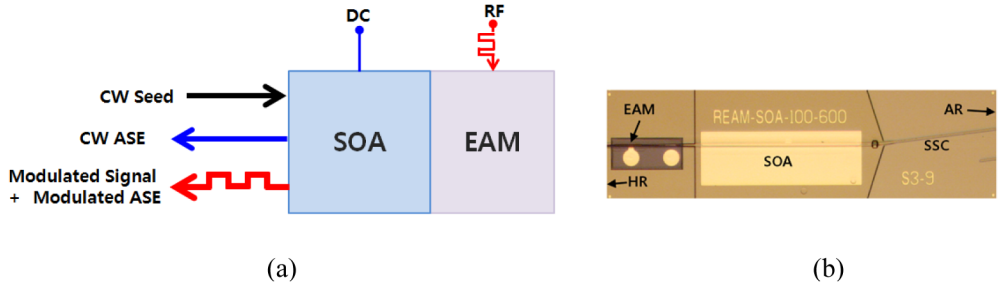

(a) (b)

Fig. 2. REAM-SOA (a) schematic view and (b) chip photograph.

3. Result and discussion

Figure 3 shows the ASE spectra of the REAM-SOA when not injecting the CW seed light and the fiber-to-fiber gain spectra when injecting the CW seed light. Figure 3(a) illustrates the ASE spectra measured at the front facet with an AR coating and at the rear facet with an HR coating when varying the bias voltage of the EAM from 0 V to 3 V in 1-V steps. The SOA current is fixed at about 100 mA. The operation temperature of the REAM-SOA is fixed into 25 °C in order to confirm the design issues. And it is considered that the seed light power is increased and the transmission distance is shorten due to thermal degradation of the REAM-SOA if the operation temperature is increased, as reported in Ref [7]. As shown in Fig. 3(a), the short-spectrum region of the ASE spectra measured at the rear facet is almost absorbed by the EAM. With increasing EAM bias, the longer ASE spectrum is decreased owing to the absorption-peak shift due to the quantum-confined Stark effect of the EAM. Through the ASE spectra of the rear facet, it is considered that the ASE light not absorbed by the REAM is returned into the SOA region after reflection by the rear facet. As shown in Fig. 3(a), the returned ASE light generates the longer-region peak in the ASE spectrum of the front facet. The longer-ASE peaks of the front facet gradually decrease with the increase of the EAM bias voltage because the amounts of returned ASE light are reduced when EAM absorption increases. On the contrary, the shorter-ASE spectra measured at the front facet are almost maintained regardless of the variation of the EAM bias voltage. The invariance of the shorter-ASE spectrum indicates that of the carrier density in the SOA. Accordingly, it is understood that the carrier depletion of the SOA is barely occurs, because the optical power of the returned ASE light is sufficiently low. It plays an important role in decreasing the input power and mitigating the pattern effect in the SOA. Figure 3(b) shows the fiber-to-fiber gain of the REAM-SOA as a function of the bias voltage of the EAM varying from 0 V to 3 V. The optical input power is fixed as −20 dBm. The center of the REAM-SOA gain appears at approximately 1585 nm, which is similar to the spectrum center of the retuned ASE light. The REAM-SOA shows the 3-dB gain bandwidth of about 30 nm with the maximum gain of

#226514 - $15.00 USD Received 7 Nov 2014; revised 15 Jan 2015; accepted 22 Jan 2015; published 28 Jan 2015

about 18 dB at the EAM bias voltage of 0 V. The static extinction ratio (ER) is greater than 15 dB between 0 V and −3 V over wavelengths ranging from 1560 nm to 1600 nm.

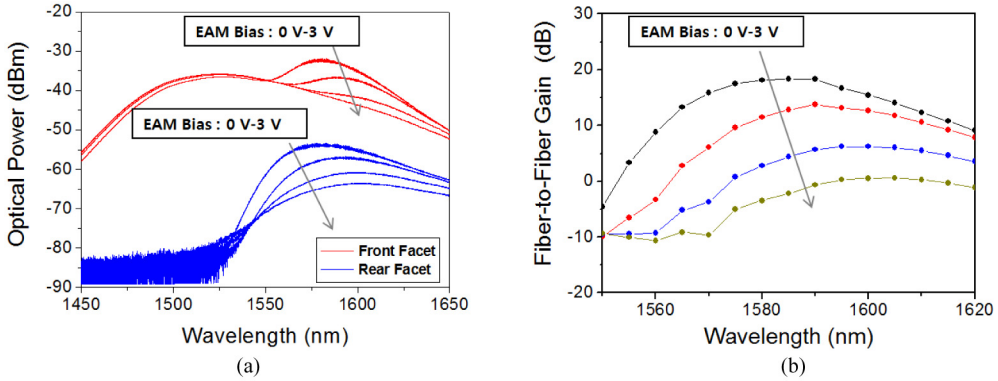

Fig. 3. (a) ASE spectra at the front facet and rear facet of REAM-SOA and (b) fiber-to-fiber gain spectra for different bias voltages of EAM.

Figure 4 shows the experimental setup used to measure the dynamic characteristics and transmission performance of the REAM-SOA for the OLT transmitter at a 10-Gb/s data rate with pseudorandom binary sequence 2^{31}–1. The TLD is used as a seed-light source. The wavelength of the TLD is set to 1585 nm, which corresponds to the gain center of the REAM-SOA. And it is estimated that the performances of the REAM-SOA over the whole L-band region appear the similar characteristics with the C-band REAM-SOA [6]. The experiments are performed with the peak-to-peak RF voltage of 1.8 $V_{p\text{-}p}$ at the bias of 1.5 V for the EAM with the bias current of 100 mA for the SOA. The optical input power of the REAM-SOA is changed from −18 dBm to 5 dBm. These operation conditions generate the optical signals with the output powers of from −6.8 dBm to 1.8 dBm and dynamic ERs of from about 8.3 dB to 9.5 dB.

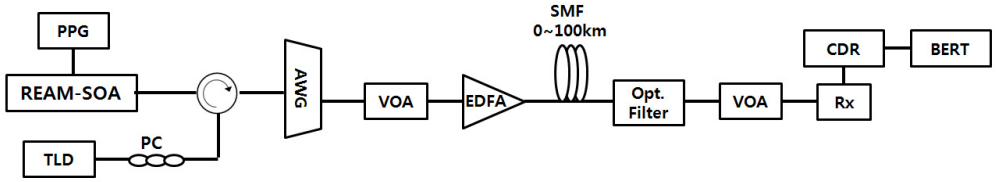

Fig. 4. Experiment setup to measure the transmission performance of 10-Gb/s REAM-SOA.

Figure 5 displays the back-to-back (BtB) bit-error-rate (BER) curves and the receiver sensitivity for varying input power. As shown in Fig. 5(a), error-free performance is achieved over a wide input power range from −16 dBm to 5 dBm. At the low input power of −18 dBm, an error-floor behavior due to the degradation of signal-to-noise ratio (SNR) is observed. Figure 5(b) shows the BtB receiver sensitivity at a BER of 10^{-9} as a function of the optical input power. According to the measurement results, the receiver sensitivity obtained is less than −22 dBm with a variation of less than 2 dB over the input power range from −16 dBm and to 5 dBm. The sensitivity increases due to the SNR degradation for low input power less than −10 dBm and due to the pattern effect for high input power of −4 dBm. These phenomena in the SOA have already been described by Watanabe et al. [15]. It is notable that the receiver sensitivity decreases when the input power is increased above −2 dBm. The sensitivity improvement at high input power is caused likely by the holding beam effect in the SOA [16]. The holding beam effect leads to the reduction of the carrier lifetime, which mitigates the pattern effect in the SOA and enhances the input power dynamic range. These

#226514 - $15.00 USD Received 7 Nov 2014; revised 15 Jan 2015; accepted 22 Jan 2015; published 28 Jan 2015

phenomena are more apparently observed at the eye patterns shown in Fig. 6. As a result, the minimum sensitivities of about −23.5 dBm are obtained at the two different input power values of −10 dBm and 2 dBm. The eye diagrams for different values of input power are shown in Fig. 6.

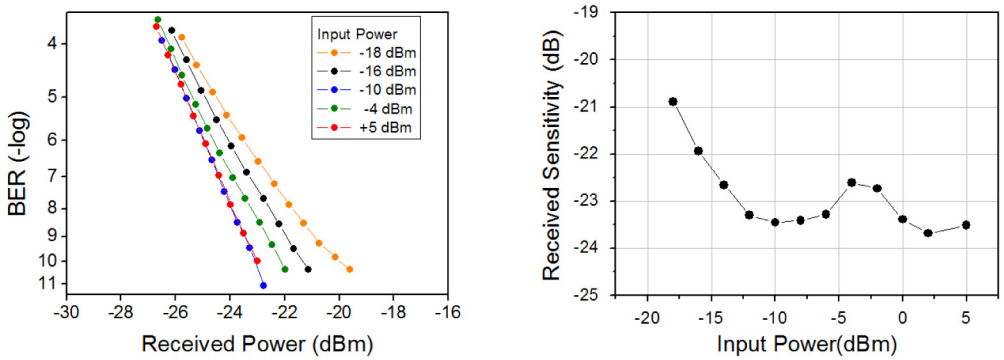

Fig. 5. (a) BtB BER curves for various input power values and (b) BtB receiver sensitivity versus input power.

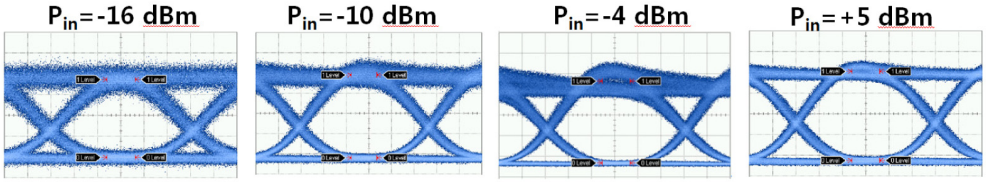

Fig. 6. 10 Gb/s eye diagrams for various input power.

The eye pattern at the low input power of −16 dBm exhibits a thicker 1-level in terms of the SNR degradation, and the eye pattern at the input power of −4 dBm shows the typical overshoot due to the pattern effect. However, the clean eye openings are obtained at both the input power values of −10 dBm and 5 dBm. The clean eye diagram at the high input power of 5 dBm can be explained by the holding beam effect in the SOA.

Figure 7 shows the measured results of BER performance for several transmission distances at the input power of −16 dBm. At the transmission distance of 50 km, we successfully demonstrated error-free operation with low power penalty of about 1.2 dB at 10^{-9} BER. Previously, the L-band REAM-SOA exhibited the power penalty of about 1.5 dB for 25 km transmission when using mode-lock laser-based multiple-wavelengths seeding light [17]. And, in the C-band REAM-SOA, the power penalty greater than 2 dB at 30 km distance was achieved with a considerably high input power of 0 dBm [5]. The BER curve at 75 km transmission shows the error-floor characteristics with the power penalty of about 4 dB. However, error-correction techniques such as forward-error correction are capable of significantly extending the transmission distance as well as lowering the input power.

Figure 8 shows the measured penalty for the transmission distances of 25 km, 50 km, and 75 km as a function of the input power at a BER of 10^{-9}. The transmission penalty at 25-km distance is negligible and is less than 0.3 dB, even exhibiting negative values resulting from the negative chirp effect in the gain saturation region of the SOA [15]. It is found that the penalty after 50-km transmission becomes less than 1.6 dB over the wide input power range from −16 dBm to 5 dBm. Meanwhile, for the transmission distance of 75 km, the power penalty rapidly increases at the input power range between −6 dBm and 2 dBm, which corresponds to the input power range having the large pattern effect, as shown in Fig. 5(b).

#226514 - $15.00 USD Received 7 Nov 2014; revised 15 Jan 2015; accepted 22 Jan 2015; published 28 Jan 2015

However, at the two different input power values of −10 dBm and 5 dBm, a low power penalty of nearly 2.6 dB is observed. It seems that the SNR improves and the pattern effect does not occur when the input power is increased to approximately −10 dBm. At a high input power of about 5 dBm, the pattern effect can be mitigated by the holding beam effect. Correspondingly, we observed the clean eye openings at the two input power values of −10 dBm and 5 dBm in the eye diagrams of Fig. 6.

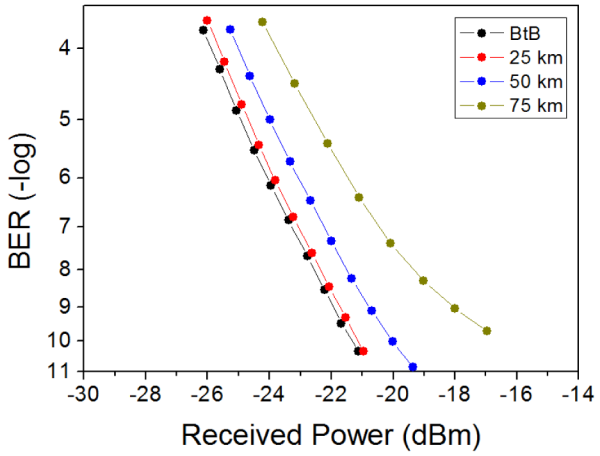

Fig. 7. BER curves for several transmission distances for an input power of −16 dBm.

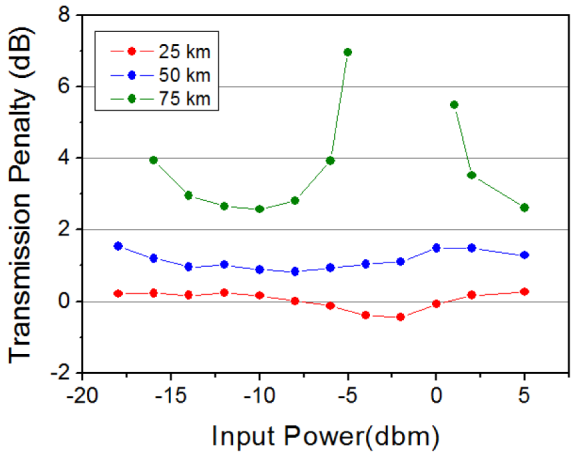

Fig. 8. Transmission penalty for several transmission distances.

Figure 9 shows the measured BER performance of the REAM-SOA for various transmission distances. At the input power of −10 dBm, as shown in Fig. 9(a), we achieve error-free performance with the transmission penalty of 2.6 dB at 75-km distance. However, the transmission over a 100-km distance shows an error-floor level of approximately 10^{-9}. As shown in Fig. 9(b), when the input power is increased to 5 dBm, the BER performance is slightly improved and the error-floor level at 100-km transmission decreases to less than 10^{-10}. It is understood that the improvement of BER performance for 100-km long reach transmission results from the pattern-effect mitigation by the holding beam effect at high input power.

#226514 - $15.00 USD Received 7 Nov 2014; revised 15 Jan 2015; accepted 22 Jan 2015; published 28 Jan 2015

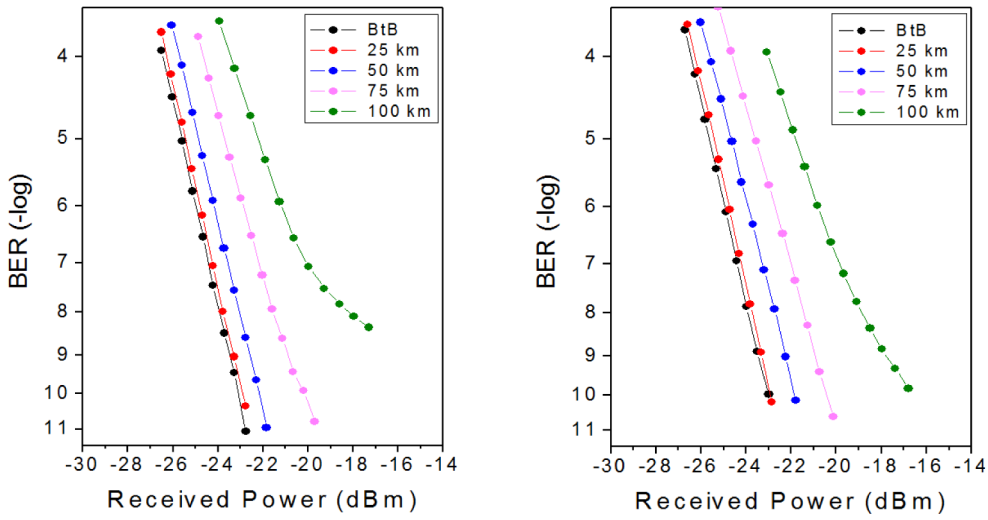

Fig. 9. BER curves up to 100-km transmission at (a) input power of −10 dBm and (b) input power of 5 dBm.

4. Conclusion

We have successfully demonstrated a 10-Gb/s L-band REAM-SOA for the OLT transmitter that extends the transmission distance with decrease of the optical input power. This extension of the transmission distance has been achieved by the reduction of the modulated ASE power returned into the SOA, which resulted from the proper wavelength deviation of the SOA ASE center wavelength and the EAM absorption peak. As a result, error-free performance has been achieved at transmission of 50 km with low penalty of 1.2 dB when lowering the input power to - 16 dBm. The power penalty at 50-km transmission was observed to be less than 1.6 dB over a wide input power range that extends from - 16 dBm to 5 dBm. Moreover, the long-reach error-free transmission over a 75-km distance has been demonstrated with a power penalty of 2.6 dB when the input power is appropriately adjusted around −10 dBm or 5 dBm. Therefore, we believe that the 10-Gb/s L-band REAM-SOA can be applied to the realization of the OLT transmitter for future long-reach access networks as it delivers reduction of size, energy, and cost of the system.

Acknowledgment

This work was supported by the ICT R&D program of MSIP, Republic of Korea. [10039164, Development of photonic integrated OLT sub-module platform for access network]

#226514 - $15.00 USD Received 7 Nov 2014; revised 15 Jan 2015; accepted 22 Jan 2015; published 28 Jan 2015